Acknowledgements

We thank G. Falkovich for theoretical guidance and discussions. The work was partially supported by the Minerva Center for Nonlinear Physics of Complex Systems, by a Research Grant from the Henry Gutwirth Fund and by an Israel Science Foundation grant.

Correspondence and requests for materials should be addressed to V.S. (e-mail: victor.steinberg@weizmann.ac.il).

Magnetic-field-induced superconductivity in a two-dimensional organic conductor

S. Uji*, H. Shinagawa*, T. Terashima*, T. Yakabe*, Y. Terai*, M. Tokumoto†, A. Kobayashi‡, H. Tanaka§ & H. Kobayashi§

** National Research Institute for Metals, Tsukuba, Ibaraki 305-0003, Japan*
† Electrotechnical laboratory, Tsukuba, Ibaraki 305-8568, Japan
‡ Research Centre for Spectrochemistry, Graduate School of Science, The University of Tokyo, Bunkyo-ku, Tokyo 113-0033, Japan
§ Institute for Molecular Science, Okazaki, Aichi 444-8585, Japan

The application of a sufficiently strong magnetic field to a superconductor will, in general, destroy the superconducting state. Two mechanisms are responsible for this. The first is the Zeeman effect[1,2], which breaks apart the paired electrons if they are in a spin-singlet (but not a spin-triplet) state. The second is the so-called 'orbital' effect, whereby the vortices penetrate into the superconductors and the energy gain due to the formation of the paired electrons is lost[3]. For the case of layered, two-dimensional superconductors, such as the high-T_c copper oxides, the orbital effect is reduced when the applied magnetic field is parallel to the conducting layers[4]. Here we report resistance and magnetic-torque experiments on single crystals of the quasi-two-dimensional organic conductor λ-$(BETS)_2FeCl_4$, where BETS is bis(ethylenedithio)tetraselenafulvalene[5–8]. We find that for magnetic fields applied exactly parallel to the conducting layers of the crystals, superconductivity is induced for fields above 17 T at a temperature of 0.1 K. The resulting phase diagram indicates that the transition temperature increases with magnetic field, that is, the superconducting state is further stabilized with magnetic field.

Studies on organic conductors have brought us deep understanding of physics in low-dimensional electronic systems. Members of the BETS family containing magnetic Fe ions among various organic conductors have been extensively studied over the past ten years because strong competition is expected between the antiferromagnetic order of the Fe moments and the superconductivity[5,6]. Of these, λ-$(BETS)_2FeCl_4$ has an unusual phase diagram, shown in Fig. 1a. At zero magnetic field, λ-$(BETS)_2FeCl_4$ shows a metal–insulator transition at 8 K (ref. 5), whereas the iso-structural salt λ-$(BETS)_2GaCl_4$ undergoes a superconducting transition around 6 K (ref. 7). The metal–insulator transition is associated with the antiferromagnetic order of the Fe moments[5,8]. The ordered Fe moments are canted by a magnetic field of about 1 T, but the electronic state remains insulating. The insulating phase is destabilized by magnetic fields above about 10 T, and a paramagnetic metallic state is then recovered.

λ-$(BETS)_2FeCl_4$ has a triclinic unit cell[6]. The planar BETS molecules are stacked along the *a* and *c* axes, and consequently form two-dimensional conduction layers (Fig. 1b). The $FeCl_4$ ion (insulating) layer is intercalated between the BETS layers, which makes the *b* axis the least conducting direction. Because of the short interatomic distance between the BETS and $FeCl_4$, finite interactions between the π (conduction) electron on the BETS molecules and the Fe^{3+} 3*d* electrons are expected. The band calculation predicts that λ-$(BETS)_2FeCl_4$ has one closed (two-dimensional) and two open Fermi surfaces in the metallic phase as shown in Fig. 1c (refs 5, 6).

The needle-like single crystals of λ-$(BETS)_2FeCl_4$, elongating along the *c* axis, were prepared by electrochemical oxidation in an appropriate solvent[6]. The resistance was measured by a conventional four-probe a.c. technique with electric current along the b^* axis, which is perpendicular to the *a*–*c* plane. Four gold wires (of diameter 10 μm) were attached to the sample by gold or carbon paint. The magnetic torque was measured by a simple cantilever technique[7]. The experiments were made with a dilution refrigerator and a 20-T superconducting magnet.

The interlayer resistance with a current *t* parallel to the b^* axis ($I_{\|b^*}$) for a magnetic field *B* parallel to the *c* axis ($B_{\|c}$) is presented in Fig. 2a. The insulator–metal transition takes place at around 10.5 T. At 0.04 K, the resistance increases with increasing field after the insulator–metal transition, has a broad maximum around 14 T, and then suddenly decreases by three orders of magnitude. Above 18 T, the detected sample voltage becomes smaller than the noise level, which suggests a superconducting phase transition. As temperature

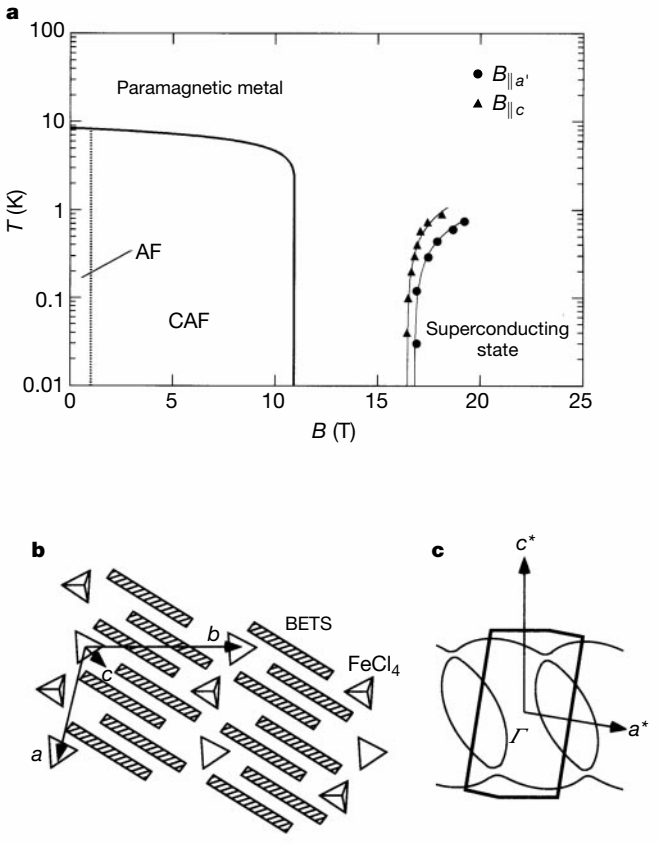

Figure 1 a, Temperature versus magnetic field phase diagram for λ-$(BETS)_2FeCl_4$ when the magnetic field is applied parallel to the *a*′ or *c* axis. At zero magnetic field, a metal–insulator transition takes place at around 8 K. In the insulating phase, the Fe moments are antiferromagnetically ordered. AF and CAF indicate the antiferromagnetic and canted antiferromagnetic phases, respectively. The superconducting phase is induced above 17 T. **b**, Schematic picture of the crystal structure of λ-$(BETS)_2FeCl_4$. The *a*–*c* plane is the conduction layer and the b axis is the least conducting axis. **c**, Calculated Fermi surfaces in the k_a–k_c plane. The area surrounded by thick lines shows the first Brillouin zone. There are one closed (two-dimensional) and two open Fermi surfaces.

increases, the sudden decrease of the resistance at high fields is suppressed and the resistance shows only monotonic increase at 1.65 K. Hysteresis is not evident at high fields above 16 T, although it is clearly observable near the insulator–metal transition. The inset shows the field-direction dependence of the resistance at three different fields, where the field is rotated in the b^*–c plane. At 14 T, the resistance is constant in this angle range, but shows a significant decrease for $B_{\|c}$ at higher fields, 17 T and 19 T. The low resistance is observed only in a very limited angle range of $|\theta| < 0.3°$.

Figure 2b shows the interlayer resistance of a different sample for B parallel to the a' ($B_{\|a'}$). The a' axis is defined as that perpendicular to both the c and b^* axes. For $B_{\|a'}$, we observe a sudden decrease of the resistance at relatively higher fields. Compared with the results for $B_{\|c}$, the resistance seems to decrease more slowly. We obtained a similar sudden decrease in resistance for four different samples. Therefore, we believe that this is intrinsic behaviour for λ-$(BETS)_2FeCl_4$. Judging from the above results, we conclude that the superconductivity is induced only when the magnetic field is parallel to the conduction layers (a–c plane).

To obtain evidence of the phase transition in thermodynamic quantities under parallel-field conditions, we measured the magnetic torque (Fig. 3). In this experiment, the sample is suspended over a conductive substrate by fine gold wires, forming a capacitor. The rotatable sample holder is mounted under very homogeneous fields (homogeneity of 10^{-4} cm^{-3}), so that the magnetic force arises only from the magnetic torque. The change in the capacitance between the sample and the substrate, that is, the sample movement, is measured as a function of magnetic field, which directly corresponds to the change in the magnetic torque[9]. To observe the finite change of the magnetic torque, the magnetic field is tilted from the a' axis by about 0.5°. In the field range where the resistance decreases steeply, we see a significant change in the magnetic torque, showing the presence of a phase transition. At 0.021 K, the torque changes at a field intensity of above 17.5 T. This change shows that the sample is moved towards the substrate by the magnetic torque when $B > 17.5$ T. The opposite change in the torque is observed when the field is tilted from the a' axis to the opposite direction. The results verify that the sample turns the a' axis toward the field direction, that is, the electronic state is more stabilized by the field parallel to the conduction layers in the high-field range. The sample maintains its position in a wider field range during the down sweep so that the field remains between the conduction layers. This behaviour suggests that the magnetic field is pinned between the superconducting layers for the down sweep. The pinning model explains why we observe a large hysteresis in the magnetic torque, but not in the resistance (Fig. 2).

We define the transition field B_c when $R/R_N = 0.5$, where R_N is the resistance in the metallic state given by extrapolating $R(B)$ from the low-field range. The transition field defined in this way corresponds to the onset of the magnetic torque change. The obtained phase diagram is presented in Fig. 1a. The transition field is slightly different for each of two field directions. Here we note two interesting features. First, the transition field seems to arise quickly at a certain field. This shows that the paramagnetic metallic state intervenes between the insulating and superconducting phases.

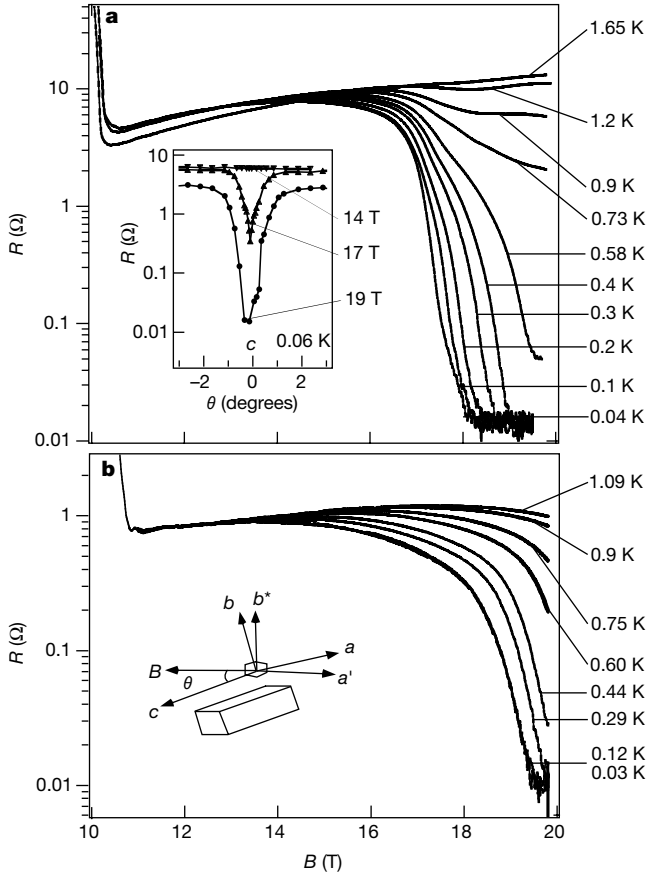

Figure 2 Interlayer resistance (for current parallel to the b^* axis) when the magnetic field is exactly parallel to the conduction layers. A steep decrease is evident at high fields, suggesting a superconducting transition. **a**, Resistance when the magnetic field is parallel to the c axis. The inset shows the field-direction dependence of the resistance under the field in the b^*–c plane. **b**, Resistance when the magnetic field is parallel to the a' axis.

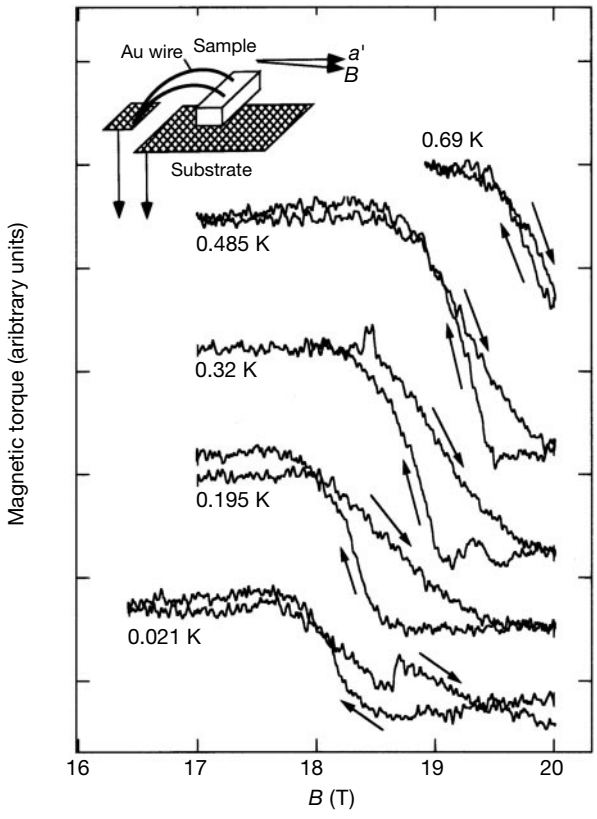

Figure 3 Magnetic torque measured by cantilever technique. The data are shifted for clarity. The inset shows the configuration of the sample and the substrate. The magnetic field is tilted from the a' axis in the a'–b^* plane by about 0.5°. A significant change associated with hysteresis, showing the presence of a phase transition, is observable at high fields.

Second, a positive curvature of the phase boundary occurs towards a high field. The positive curvature suggests that the transition field increases with temperature.

Field-induced superconductivity has been reported for paramagnetic $Eu_xSn_{1-x}Mo_6S_8$ (ref. 10). This material is a superconductor with $T_c = 3.8$ K. As the magnetic field increases, the superconductivity is restored above 4 T and below 0.1 K, after it is destroyed at about 1 T. This phenomenon is well understood in terms of the Jaccarino–Peter compensation effect[11]; the internal magnetic field created by the Eu moments through the exchange interaction is compensated by the external magnetic field. For λ-$(BETS)_2FeCl_4$, because an exchange interaction between the Fe moments and the conduction electrons is expected, the Jaccarino–Peter compensation effect may be a possible mechanism. However, this effect cannot explain how a very small amount of the magnetic field (at about 0.1 T) along the b^* axis destroys the superconducting state, because the paramagnetic Fe moments are aligned along the external field irrespective of the field direction. The surprisingly strong anisotropic superconducting transition for λ-$(BETS)_2FeCl_4$ suggests that the low dimensionality of the electronic system is closely related to the mechanism of the superconductivity.

For quasi-two-dimensional electronic systems such as λ-$(BETS)_2FeCl_4$, when a high magnetic field is applied exactly parallel to the conduction layers, the motion of the electrons is confined onto a single conduction layer. This is field-induced dimensional crossover from quasi-two-dimensional to two-dimensional. In this case, the orbital effect, one of the mechanisms destroying the superconductivity, is largely suppressed. However, if even a small amount of the magnetic field is perpendicular to the conduction layers, the electrons drift in the interlayer direction and the orbital effect is restored. This picture of dimensional crossover seems consistent with the experimental observation that very low magnetic fields along the b^* axis destroy superconductivity (Fig. 2a). On the basis of the dimensional crossover, various theoretical models predicting the existence of high-field superconducting phases have been proposed[12–16]. However, all the theories tacitly assume that the superconductivity is stable at zero field.

The superconductivity of the iso-structural salt λ-$(BETS)_2GaCl_4$ ($T_c = 6$ K) survives in a magnetic field of up to 5 T that is perpendicular to the conduction layers[17]. This field is much larger than that for λ-$(BETS)_2FeCl_4$ (at about 0.1 T). We have carefully measured the resistance for λ-$(BETS)_2GaCl_4$ under fields exactly parallel to the conducting layers, but superconductivity was not restored at fields up to 20 T after the superconductivity was destroyed at around 13 T. The completely different phase diagrams of λ-$(BETS)_2GaCl_4$ and λ-$(BETS)_2FeCl_4$ suggest that the interaction between the Fe moments and the conduction electrons, as well as the low dimensionality of the electronic system, strongly affects the emergence of the superconductivity. It seems likely that the pairing interaction between the π electrons on the BETS molecules arises from the magnetic fluctuation through the paramagnetic Fe moments. □

Received 6 December 2000; accepted 14 February 2001.

1. Chandrasekhar, B. S. A note on the maximum critical field of high-field superconductors. *Appl. Phys. Lett.* **1,** 7–8 (1962).
2. Clogston, A. M. Upper limit for the critical field in hard superconductors. *Phys. Rev. Lett.* **15,** 266–267 (1962).
3. Tinkham, M. *Introduction to Superconductivity* (McGraw-Hill, New York, 1975).
4. Klemm, R. A., Luther, A. & Beasley, M. R. Theory of the upper critical field in layered superconductors. *Phys. Rev. B* **12,** 877–891 (1975).
5. Brossard, L. *et al.* Interplay between chains of S = 5/2 localised spins and two-dimensional sheets of organic donors in the synthetically built magnetic multilayer λ-$(BETS)_2FeCl_4$. *Eur. Phys. J. B* **1,** 439–452 (1998).
6. Kobayashi, H. *et al.* New BETS conductors with magnetic anions (BETS=bis(ethylenedithio)tetraselenafulvalene). *J. Am. Chem. Soc.* **118,** 368–377 (1996).
7. Kobayashi, H. *et al.* Electric and magnetic properties and phase diagram of a series of organic superconductors λ-$(BETS)_2GaX_ZY_{1-z}$ [X, Y=F, Cl, Br; $0 < z < 2$]. *Phys. Rev. B* **56,** R8526–R8529 (1997).
8. Akutsu, H. *et al.* Highly correlated organic conductor with magnetic anions exhibiting a π-d coupled metal-insulator transition, λ-$(BETS)_2FeBr_xCl_{1-x}$. *J. Am. Chem. Soc.* **119,** 12681–12682 (1997).
9. Brooks, J. S., Naughton, M. J., Ma, Y. P., Chaikin, P. M. & Chamberlin, R. V. Small sample magnetometers for simultaneous magnetic and resistive measurements at low temperatures and high magnetic fields. *Rev. Sci. Instrum.* **58,** 117–121 (1987).
10. Meul, H. W. *et al.* Observation of magnetic-field-induced superconductivity. *Phys. Rev. Lett.* **53,** 497–500 (1984).
11. Jaccarino, V. & Peter, M. Ultra-high-field superconductivity. *Phys. Rev. Lett.* **9,** 290–292 (1962).
12. Lebed, A. G. Reversible nature of the orbital mechanism for the suppression of superconductivity. *JETP Lett* **44,** 114–117 (1986).
13. Dupuis, N., Montambaux, G. & Sa de Melo, C. A. R. Quasi-one-dimensional superconductors in strong magnetic field. *Phys. Rev. Lett.* **70,** 2613–2616 (1993).
14. Miyazaki, M., Kishigi, K. & Hasegawa, Y. Superconductivity of quasi-one- and quasi-two-dimensional tight binding electrons in a magnetic field. *J. Phys. Soc. Jpn* **67,** 2618–2621 (1998).
15. Shimahara, H. Coexistence of singlet and triplet attractive channels in the pairing interactions mediated by antiferromagnetic fluctuations. *J. Phys. Soc. Jpn* **69,** 1966–1969 (2000).
16. Sa de Melo, C. A. R. Paramagnetism and reentrant behaviour in quasi-one-dimensional superconductors at high magnetic fields. *Physica C* **260,** 224–230 (1996).
17. Tanatar, M. A. *et al.* Anisotropy of the upper critical field of the organic conductor λ-$(BETS)_2GaCl_4$. *J. Supercond.* **12,** 511–514 (1999).

Correspondence and requests for materials should be addressed to S.U. (e-mail: uji@nrim.go.jp).

Solid acids as fuel cell electrolytes

Sossina M. Haile, Dane A. Boysen, Calum R. I. Chisholm & Ryan B. Merle

Materials Science, California Institute of Technology, Pasadena, California 91125, USA

Fuel cells are attractive alternatives to combustion engines for electrical power generation because of their very high efficiencies and low pollution levels. Polymer electrolyte membrane fuel cells are generally considered to be the most viable approach for mobile applications. However, these membranes require humid operating conditions, which limit the temperature of operation to less than 100 °C; they are also permeable to methanol and hydrogen, which lowers fuel efficiency. Solid, inorganic, acid compounds (or simply, solid acids) such as $CsHSO_4$ and $Rb_3H(SeO_4)_2$ have been widely studied because of their high proton conductivities and phase-transition behaviour. For fuel-cell applications they offer the advantages of anhydrous proton transport and high-temperature stability (up to 250 °C). Until now, however, solid acids have not been considered viable fuel-cell electrolyte alternatives owing to their solubility in water and extreme ductility at raised temperatures (above approximately 125 °C). Here we show that a cell made of a $CsHSO_4$ electrolyte membrane (about 1.5 mm thick) operating at 150–160 °C in a H_2/O_2 configuration exhibits promising electrochemical performances: open circuit voltages of 1.11 V and current densities of 44 mA cm^{-2} at short circuit. Moreover, the solid-acid properties were not affected by exposure to humid atmospheres. Although these initial results show promise for applications, the use of solid acids in fuel cells will require the development of fabrication techniques to reduce electrolyte thickness, and an assessment of possible sulphur reduction following prolonged exposure to hydrogen.

Solid acids are compounds such as $KHSO_4$ whose chemistry and properties lie between those of a normal acid (such as H_2SO_4) and a normal salt (such as K_2SO_4)[1]. They are typically comprised of oxyanions—for example, SO_4 or SeO_4—that are linked together via O–H···O hydrogen bonds. Within this category the $MHXO_4$ and $M_3H(XO_4)_2$ compounds, where M = Cs, NH_4, Rb, and X = S or Se, are known to undergo a "superprotonic" phase transition[2–9]. On passing through the transition the conductivity jumps by several orders of magnitude to a value of 10^{-3} to 10^{-2} Ω^{-1} cm^{-1}, and the